Journal of Solid State Chemistry **156,** 422–427 (2001)
doi:10.1006/jssc.2000.9017, available online at http://www.idealibrary.com on IDEAL®

Crystal Growth, Structure, and Transport Properties of the Five-Leg Spin Ladder Compound $La_8Cu_7O_{19}$

C. Sekar,[1] T. Watanabe, A. Matsuda, and H. Shibata

NTT Basic Research Laboratories, 3-1 Wakamiya Morinosato, Atsugi-shi, Kanagawa 243-0198, Japan

and

Y. Zenitani and J. Akimitsu

Department of Physics, Aoyama Gakuin University, 6-16-1 Chitosedai, Setagaya-ku, Tokyo 157-8572, Japan

Received July 5, 2000; in revised form October 13, 2000; accepted October 27, 2000

The crystallization region of $La_8Cu_7O_{19}$ exists in a narrow temperature (1045–1050°C) and composition range (1:4.5–1:5.0; La_2O_3:CuO molar ratio) in the La_2O_3–CuO system in an air ambient. In this narrow range, we have succeeded in growing large $La_8Cu_7O_{19}$ single crystals, for the first time, by a modified slow cooling method. Single-crystal X-ray diffraction analysis reveals that $La_8Cu_7O_{19}$ crystallizes in a monoclinic structure with space group $C2/c$ and has the lattice parameters $a = 13.82(7)$ Å, $b = 3.734(8)$ Å, $c = 34.77(10)$ Å, and $\beta = 99.3(4)^\circ$. The electrical transport behavior of the as-grown and hole-doped $La_8Cu_7O_{19}$ single crystals are semiconducting. A lowest resistivity of 11.0 mΩ-cm is measured at 293 K along the ladder direction ($\|b$-axis) for the hole-doped samples. © 2001 Academic Press

Key Words: **spin ladder; $La_8Cu_7O_{19}$ single crystals; structure; transport property.**

1. INTRODUCTION

The study of spin ladders, composed of $S = \frac{1}{2}$ antiferromagnetically coupled chains, has been emerging as one of the active areas of research in the field of high-Tc superconductivity. It is now well known that the ladders with even and odd number of legs have quite generic features, such as the presence of a spin gap at half-filling in even-leg systems and its absence in odd-leg ladders (1). The possibility of superconductivity has been predicted for an even-leg ladder system lightly doped with holes (1) and, subsequently, the two-leg ladder compound $(Sr_{0.4}Ca_{13.6})_{14}Cu_{24}O_{41}$ was discovered to be superconducting at 12 K under high pressure of 3 GPa (2). In the case of odd-leg ladders, it has been predicted that they might exhibit properties similar to single chains at low energies (1). It has been experimentally proved that the magnetic properties of the well-known odd-leg ladder compound $Sr_2Cu_3O_5$ (three-leg) are consistent with the theoretical predictions (3). However, this compound could be synthesized only under high pressure and also hole-doping is difficult. Hence, transport properties have not been studied.

The compound $La_8Cu_7O_{19}$, $n = 3$ member of the new homologous series of lanthanum cuprates $La_{4+4n}Cu_{8+2n}O_{14+8n}$, consists of five-legs, and it is also asserted to lack a spin gap in its magnetic excitation spectrum (4, 5). Recently, Zenitani *et al.* (6) succeeded in hole-doping polycrystalline $La_8Cu_7O_{19}$ by means of high-oxygen-pressure annealing using a hot-isostatic-pressing (HIP) furnace. A significant decrease in the resistivity was observed in those samples, although no transition was observed from the semiconducting behavior. Single crystals are more suitable for studying both the doping effect and the anisotropic properties. However, there have been no reports on crystal growth because $La_8Cu_7O_{19}$ was thought to have no temperature interval where $La_8Cu_7O_{19}$ could exist in equilibrium with the liquidus (4, 7). During the course of our recent attempts to crystallize $La_2Cu_2O_5$ (four-leg), $n = 2$ member of the same homologous series, we found that in ambient air the $La_8Cu_7O_{19}$ cocrystallizes with $La_2Cu_2O_5$ (as mixed crystals) in a small temperature interval between 1045 and 1050°C (8). This very narrow equilibrium range makes it difficult to crystallize $La_8Cu_7O_{19}$ by a standard slow cooling (SSC) method. In this paper, the preparation of $La_8Cu_7O_{19}$ single crystals by a modified slow cooling method and characterization of those crystals with respect to their structure, elemental composition, and transport properties are presented.

[1] To whom correspondence should be addressed. Fax: +81-46-240-4722. E-mail: sekar@with.brl.ntt.co.jp.

0022-4596/01 $35.00

2. EXPERIMENTAL

Single crystals of $La_8Cu_7O_{19}$ were grown using a modified slow cooling (MSC) technique. In this method, a flux-poor starting compound is subjected to a rapid cooling from high temperature ($\sim$1300°C) to the appropriate crystallization temperature (Ts) to produce a highly supersaturated solution and to avoid the formation of high-temperature-phase La_2CuO_4. The starting charge for crystal growth was prepared by mixing $La_8Cu_7O_{19}$ powder (sintered in air at 1020°C) and CuO in the appropriate molar ratio (La_2O_3 : CuO) and ground well using a mechanical mortar. The charge ($\sim$60 g) was then placed in a Pt crucible (100 cm^3) and loaded in to a vertical box-type furnace with open SiC heating elements. The furnace temperature was raised to 1300°C in 5 h, soaked for about 3–5 h, and then rapidly cooled to Ts in about 10 min. Slow cooling was effected from Ts to 1010°C at a rate of 0.5–1°C/h, followed by furnace cooling to room temperature. A number of experiments were carried out for different starting compositions between 1:4.5 and 1:5.0 and soak temperatures (Ts) between 1045 and 1050°C. A few growth runs were also carried out using CuO-rich starting compositions both by SSC and MSC. The loss of the material due to evaporation during MSC growth was found to be within 4 wt%.

Phase purity and crystallinity of the as-grown crystals were studied by X-ray diffraction method. The elemental (La/Cu) composition of the crystal was measured by electron probe microanalysis (EPMA). Measurement at several points of the same high-purity $La_8Cu_7O_{19}$ crystal confirmed the composition, and also no impurity phase was detected. Contamination of the crystals by Pt (from the crucible) was found to be of the order of the detection limit of the EPMA measurement (< 0.5 at.%). Temperature-dependent electrical resistivity (ρ–T) was measured by the standard four-probe method. High-oxygen-pressure annealing was carried out at 600°C under a pressure of 400 atm (20% O_2 + 80% Ar at a total pressure of 2000 atm) using the HIP furnace.

3. RESULTS AND DISCUSSION

3.1. Crystal Growth

Although $La_8Cu_7O_{19}$ is reported to have been prepared in a single phase in oxygen atmosphere (4), we could not crystallize $La_8Cu_7O_{19}$ in flowing oxygen and also under high-pressure oxygen [$P(O_2) = 3$–9 atm] atmospheres (8). Instead, under these conditions, we have succeeded in growing high-purity $La_2Cu_2O_5$ single crystals from a wide range of starting compositions between 1:5.25 and 1:3.75 (Ref. 8). Contrary to this, in ambient air, $La_8Cu_7O_{19}$ phase has been found to crystallize in a mixed crystal form [$La_2Cu_2O_5$ + $La_8Cu_7O_{19}$] in a very narrow composition (1:4.5–1:5.0) and temperature (1045 and 1050°C) ranges. However, even in air, a CuO-rich melt (≤ 6.0 CuO) results in pure $La_2Cu_2O_5$ crystals irrespective of the growth method (i.e., both SSC and MSC). Experimental details of SSC are described in Ref. 8. In the present work, we have attempted to grow phase-pure $La_8Cu_7O_{19}$ single crystals from the flux-poor starting compositions.

Our initial attempts to grow $La_8Cu_7O_{19}$ crystals (starting charges 1:4.5–1:5.0) by standard slow cooling were not successful. The resulting partial melt contained only a number of micrometer-sized crystals. However, powder X-ray analyses indicated that the crystallites were mainly the $La_2Cu_2O_5$ phase, although, in some cases, mixed phases were also observed. The possible reason could be the nonavailability of sufficient supersaturation for crystallization of $La_8Cu_7O_{19}$ when the melt passes through the narrow liquidus line. Figures 1a and 1b show X-ray diffraction patterns of mixed crystals grown by MSC. Note that the crystal grown from a 1:5.0 ratio has a major $La_8Cu_7O_{19}$ phase. Crystal growth from the 1:4.5 ratio has yielded mostly a mixture of pure $La_2Cu_2O_5$ and mixed ($La_2Cu_2O_5$ + $La_8Cu_7O_{19}$) crystals.

In the subsequent runs, for a fixed starting composition of 1 : 5, we did a number of growth runs at different crystallization temperatures (Ts), and 1047°C was found to be the optimum value. At higher Ts (> 1052°C), square-shaped La_2CuO_4 crystals and a few bar-shaped mixed crystals were found to have grown inside the melt. With the decrease in Ts, the proportion of $La_2Cu_2O_5$ increases, reaching almost pure $La_2Cu_2O_5$ around 1042°C. At the optimized Ts (1047°C), we were able to grow almost pure $La_8Cu_7O_{19}$ crystals. As-grown crystals have had thick bar-shaped morphology with shiny surfaces. However, single crystal X-ray analysis revealed that the crystals contained traces of $La_2Cu_2O_5$ impurity. Based on the experimental

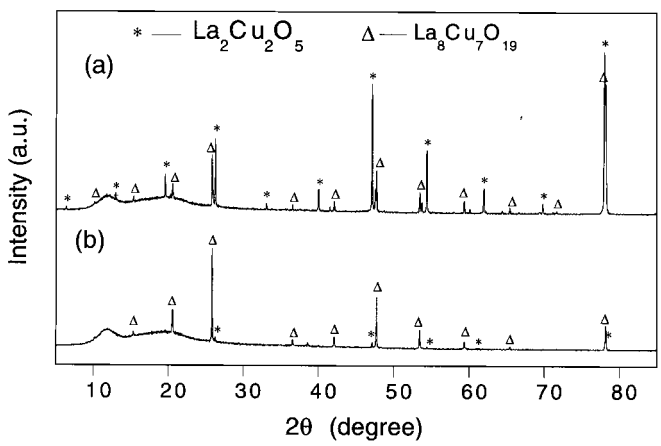

FIG. 1. XRD pattern of crystals grown from two different starting compositions [La_2O_3 : CuO; molar ratio] and crystallization temperatures: (a) 1:4.5, 1045°C; (b) 1:5.0, 1050°C.

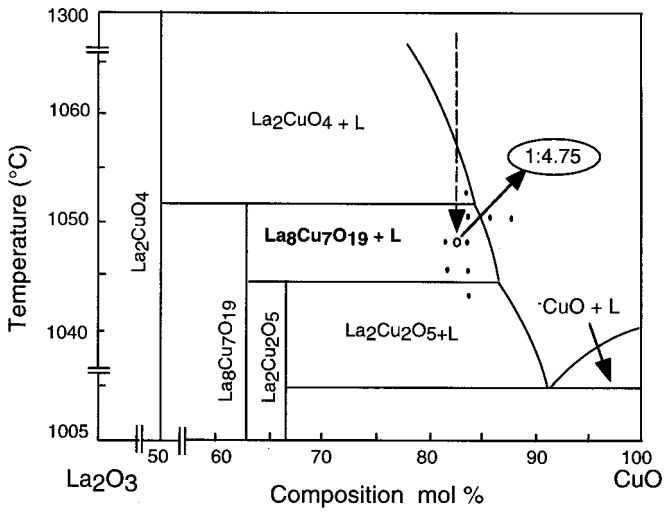

FIG. 2. Schematic representation of the quasi-binary phase diagram of the La_2O_3–CuO system in air. Black circles represent the experimental points. The dashed arrow indicates the rapid cooling from high temperature to the crystallization temperatures.

observations, we drew a schematic quasi-binary phase diagram of the La_2O_3–CuO system, which is shown in Fig. 2.

The phase diagram suggests that the supersaturation can further be enhanced by choosing a still slightly poor CuO region (< 5.0). Accordingly, in order to improve the phase purity, we further studied different starting compositions and found 1:4.75 to be the most appropriate one for a fixed Ts of 1047°C. Thus obtained crystals have no impurity phases as confirmed by XRD analysis (Fig. 3a). Further decrease in the CuO ratio, however, did not yield good crystals. This could be attributed to the excessive inequilibrium between the solute and the solvent that results from the poor-CuO starting composition and also to the loss of CuO due to evaporation ($\sim$4–5 wt%).

Thus, a systematic study of the La_2O_3–CuO phase diagram enabled us to grow high-purity $La_8Cu_7O_{19}$ single crystals. The open circle in phase diagram marks the optimum temperature and composition values (Fig. 2). Under these optimized conditions, two types of crystals were obtained from the same batch. The first type of crystals have thin bar-shaped morphology (with sizes up to $0.15 \times 2.8 \times 0.05$ mm^3), which grew like druses on the surface of the melt (type I). The second type, which have fairly thick bar-shaped morphology (with sizes up to $0.12 \times 1.5 \times 0.2$ mm^3), were found inside the melt (type II). All the type I crystals were found to be high-purity $La_8Cu_7O_{19}$, as shown in Fig. 3a. The full-width at half-maximum (HWFM) of a rocking curve for the (0, 0, 14) diffraction peak is typically 0.024°, which demonstrates the very good crystallinity of the sample (Fig. 3b). Further XRD studies on a number of type II crystals indicated that some of them have traces of $La_2Cu_2O_5$ impurity. This could be due to decrease in supersaturation with the continuous growth of $La_8Cu_7O_{19}$ crystals. In this situation, it is highly probable that the $La_2Cu_2O_5$ nucleates and grows as an impurity in the $La_8Cu_7O_{19}$ crystal. These results may reflect the fact that the liquidus line of $La_8Cu_7O_{19}$ is very narrow, as shown in Fig. 2. An alternative interpretation is that the $La_8Cu_7O_{19}$ phase may exist only in inequlibrium with the liquidus.

3.2. *Single-Crystal X-Ray Analysis*

A crystal of $La_8Cu_7O_{19}$ was examined using a four-circle X-ray diffractometer (RIGAKU) equipped with a Mo$K\alpha$ radiation source. Experimental conditions for data collection and refinement are given in Table 1. All structural calculations have been done with the TEXSAN program (Structure Analysis Software, Molecular Structure Corporation (1996)). Absorption correction was made using the Ψ-scan method. The starting structural model was constructed by the heavy atom method. Then the refinements using a least squares calculation were done. The results indicate that $La_8Cu_7O_{19}$ crystallizes in a monoclinic structure with space group $C2/c$ and has the lattice parameters

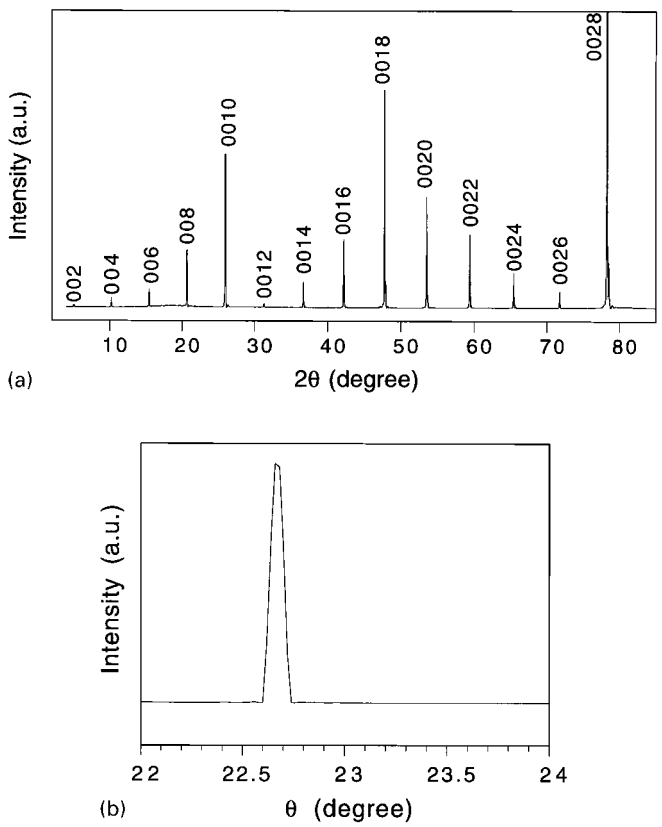

FIG. 3. (a) XRD pattern of a typical high-purity $La_8Cu_7O_{19}$ single crystal [starting composition, 1:4.75 (La_2O_3:CuO; molar ratio); crystallization temperature, 1047°C]. (b) Rocking curve of the same crystal.

TABLE 1
Data Collection Parameters of $La_8Cu_7O_{19}$

Crystal size	$0.2 \times 0.4 \times 0.8\ mm^3$
Temperature	293 K
Crystal system	Monoclinic
Space group	$C2/c$ (unique axis b)
a	13.82(7) Å
b	3.734(8) Å
c	34.77(10) Å
β	99.3(4)°
Volume	1770(15) $Å^3$
Z	4
Calculated density	6.98 g/cm^3
Absorption coefficient μ (Mo$K\alpha$)	202.9 mm^{-1}
Min. transm.	0.001
Max. transm.	0.583
Scan mode	ω
$2\theta_{max}$	55.1°[Mo$K\alpha$ ($\lambda = 0.70926$ Å)]
Measured reflections	2420
Unique reflections	2335
Observed reflections (F_{obs} (hkl) > 3.0 $\sigma F(hkl)$ in L.S.)	1673
Parameters	107
Refinement method	Full-matrix least squares on $\|F\|$
$R(F)$	0.075
$Rw(F)$	0.094
Extinction length	0.86(1) μm

Note. The standard deviations are given in parentheses as errors in the last significant digit.

$a = 13.82(7)$ Å, $b = 3.734(8)$ Å, $c = 34.77(10)$ Å, and $\beta = 99.3(4)°$, with cell volume $V = 1770(15)$ $Å^3$. The refinement of the crystal structure gave an R-factor of 0.075 and Rw of 0.094, which confirm the good crystallinity. The crystal structure and the lattice parameters are consistent with the previous results for polycrystalline samples (4). Figure 4 shows the crystal structure of $La_8Cu_7O_{19}$, the unit cell of which is enclosed in a box. The basic structural unit (subcell) consists of three-octahedra-wide La_2CuO_4 block and Cu–O planes of complex geometry. An inclined out-of-plane axis (i.e., "c" axis) of La_2CuO_4 blocks positions along the a axis of $La_8Cu_7O_{19}$. The complex copper–oxygen planes consist of a double Cu–O chain running parallel to the b-axis, similar to the double chain found in $YBa_2Cu_4O_8$, and pairs of distorted CuO_4 tetrahedra sharing a common edge, and sharing corners with the double chains. Actually, the CuO diamonds in the double chains are puckered to the extent that they could be treated as flattened tetrahedra. Considering the above structural features, the combination of three Cu–O chains in the La_2CuO_4 blocks and two Cu–O chains of double chains at the width of the La_2CuO_4 blocks could be regarded as the five legs of the ladder structure. Basically, $La_8Cu_7O_{19}$ crystallizes in the same structure as $La_2Cu_2O_5$ (four-leg), $n = 2$ member of the homologous series $La_{4+4n}Cu_{8+2n}O_{14+8n}$, except for the number of legs.

The atomic positions and thermal parameters of $La_8Cu_7O_{19}$ are assigned (Table 2) following the notations used by Cava *et al.* (4). Interatomic distances between lanthanum–oxygen bonds and a few selected copper–oxygen bond lengths are listed in Table 3. The Jahn-Teller distortion of the copper–oxygen octahedron in $La_8Cu_7O_{19}$ is similar to that in La_2CuO_4 with in-plane distances near 1.92 Å and apical oxygen bond lengths near 2.42 Å. Similar results have been reported for $La_2Cu_2O_5$ (4). However, closer observation of bond lengths indicates that the "rung" lengths (of the ladder structure) at the octahedral sites of $La_8Cu_7O_{19}$ are shorter (1.915 Å) than in $La_2Cu_2O_5$ (1.950 Å). This is in agreement with the fact that, in the as-synthesized state, $La_8Cu_7O_{19}$ is doped with more hole carriers compared to $La_2Cu_2O_5$. The bond lengths of the four-coordinated copper (Cu3) in the puckered double chains of $La_8Cu_7O_{19}$ are larger (2.018 Å) than those of the corresponding Cu2 sites in $La_2Cu_2O_5$ (1.972 Å). However, in both cases, tetrahedral copper (Cu4 for $La_8Cu_7O_{19}$ and

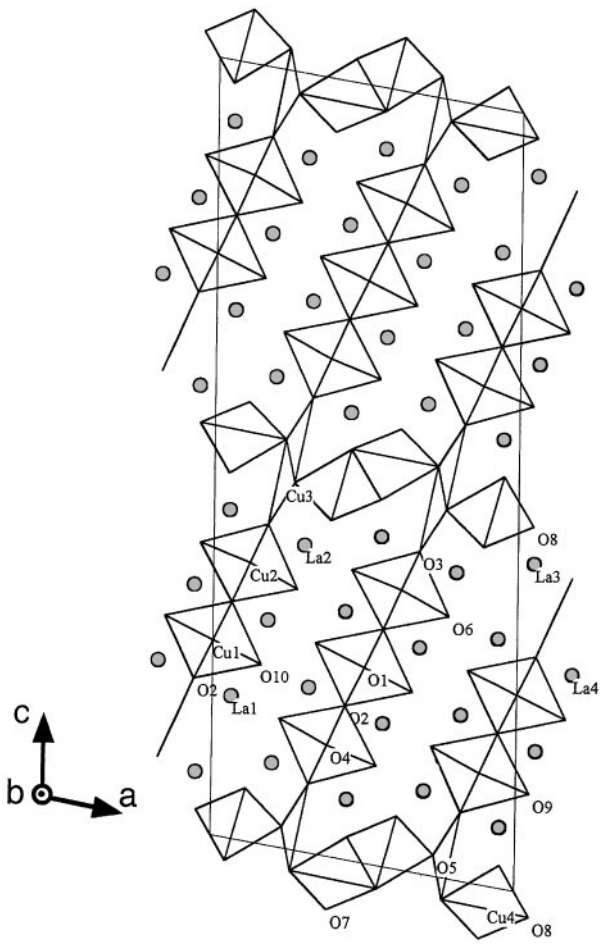

FIG. 4. The crystal structure of $La_8Cu_7O_{19}$ in the a–c plane. Atomic positions of La, Cu, and O are shown. The unit cell is enclosed in a box.

TABLE 2
Atom Positions and Thermal Parameters of $La_8Cu_7O_{19}$

Atom	site	x	y	z	B_{iso} (Å^2)
La1	8*f*	0.4365(1)	0.9746(1)	0.3175(1)	0.43(1)
La2	8*f*	0.2996(1)	0.4636(1)	0.3938(1)	0.44(1)
La3	8*f*	0.5520(1)	0.0077(1)	0.4227(1)	0.51(1)
La4	8*f*	0.1814(1)	0.4800(1)	0.2885(1)	0.45(1)
Cu1	4*e*	0.5000(0)	0.4727(5)	0.2500(0)	0.31(2)
Cu2	8*f*	0.7344(1)	0.4811(3)	0.3578(1)	0.40(1)
Cu3	8*f*	0.5858(1)	0.5101(4)	0.4962(1)	0.68(2)
Cu4	8*f*	0.0859(1)	0.3764(3)	0.5227(1)	0.50(2)
O1	4*e*	0.5000(1)	0.9775(34)	0.2500(1)	1.21(17)
O2	8*f*	0.5615(3)	0.4677(19)	0.3035(1)	0.08(9)
O3	8*f*	0.6784(4)	0.4916(20)	0.4124(1)	0.41(10)
O4	8*f*	0.6198(4)	0.9851(21)	0.3583(1)	0.73(10)
O5	8*f*	0.7356(5)	0.4779(25)	0.5273(2)	1.50(13)
O6	8*f*	0.7770(4)	0.4567(19)	0.3350(1)	0.77(9)
O7	8*f*	0.6133(5)	0.0598(23)	0.5675(2)	1.15(12)
O8	8*f*	0.5491(4)	0.5322(21)	0.4707(1)	0.57(10)
O9	8*f*	0.4599(4)	0.4489(22)	0.3731(1)	0.78(12)
O10	8*f*	0.3395(4)	0.4539(21)	0.2703(1)	0.64(0)

Note. The standard deviations are given in parentheses as errors in the last significant digit.

Cu3 for $La_2Cu_2O_5$) between the chains display similar Cu–O bond lengths of about 1.96 Å.

3.3. Electrical Transport Property

Figure 5 shows the temperature-dependent electrical resistivity behavior of a typical $La_8Cu_7O_{19}$ single crystal along its ladder direction (||*b*-axis). The room-temperature resistivity of the as-grown crystal is 1.90 ohm cm, which is much lower than that of the $La_2Cu_2O_5$ crystal [1.70×10^3 ohm-cm for as-grown crystals (8)]. The observed low resistivity suggests that as-grown $La_8Cu_7O_{19}$ crystal is slightly doped with carriers compared to $La_2Cu_2O_5$. A significant drop in the resistivity (11.0 mohm cm at 293 K) was observed for the crystals annealed under high oxygen pressure of 400 atm at 600°C for an extended period of about 23 days. However, no transition is observed in the semiconducting behavior. An anomaly observed in the ρ-T behavior for a particular level of doping may be attributed to inhomogeneous oxygen distribution in the crystal or it may be related to some kind of charge ordering, as suggested in the resistivity measurement of $Sr_{14}Cu_{24}O_{41}$ (9). Further hole-doping and anisotropic measurements are needed for a complete understanding of the transport behavior of $La_8Cu_7O_{19}$.

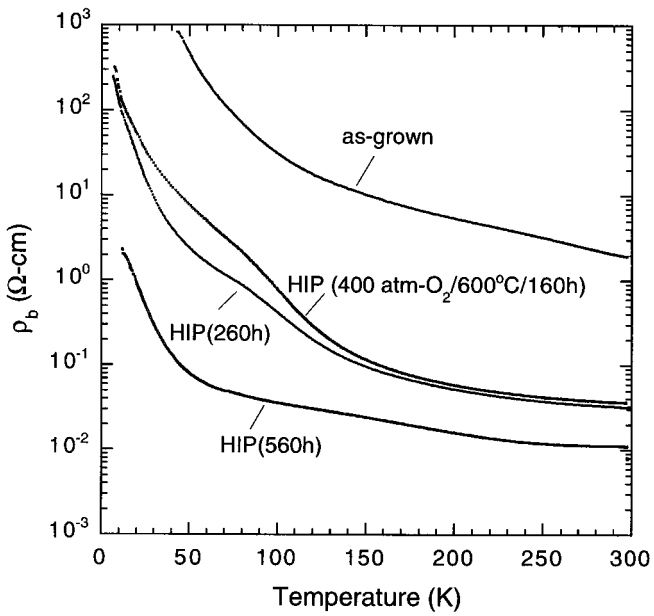

FIG. 5. Resistivity–temperature curves of a $La_8Cu_7O_{19}$ single crystal along the ladder direction (||*b*)

4. CONCLUSIONS

Conditions for the growth of large, high-quality $La_8Cu_7O_{19}$ single crystals have been optimized and crystals

TABLE 3
Principal Interatomic Distances in $La_8Cu_7O_{19}$

La1–O1	2.637(4)	La4–O1	2.642(6)
–O2	2.658(7)	–O2	2.641(7)
–O2	2.627(7)	–O2	2.569(7)
–O4	2.694(7)	–O4	2.700(4)
–O6	2.382(3)	–O6	2.730(9)
–O9	2.734(7)	–O6	2.618(9)
–O9	2.606(7)	–O10	2.372(3)
–O10	2.730(9)	–O10	2.793(7)
–O10	2.731(9)		
La2–O3	2.588(7)	Cu1–O1	1.849(1)
–O3	2.729(7)	–O1	1.885(1)
–O3	2.872(2)	–O2	1.915(4)
–O4	2.589(6)	–O10	2.435(3)
–O6	2.728(7)		
–O6	2.769(7)	Cu2–O2	1.929(4)
–O7	2.555(8)	–O3	1.939(4)
–O7	2.433(8)	–O4	1.882(1)
–O9	2.386(3)	–O6	2.431(3)
		–O9	2.414(2)
		Cu3–O3	2.002(4)
La3–O3	2.661(7)	–O5	1.867(2)
–O3	2.581(6)	–O5	1.957(2)
–O4	2.566(4)	–O5	2.021(1)
–O7	2.378(2)		
–O8	2.439(6)	Cu4–O5	2.086(2)
–O8	2.580(6)	–O7	1.941(5)
–O9	2.585(9)	–O8	1.944(2)
–O9	2.894(9)	–O8	1.887(4)

Note. The standard deviations are given in parentheses as errors in the last significant digit.

have been grown by a novel modified slow cooling technique from an inequilibrium initial condition. X-ray diffraction and elemental analyses confirmed the good crystallinity and high purity of the grown crystals. Single crystal X-ray analysis confirmed the basic crystal structure (proposed by Cava et al. using polycrystal data) and yields detailed crystallographic parameters for $La_8Cu_7O_{19}$. These are compared with those of $La_2Cu_2O_5$. Temperature-dependent resistivity measurements along the ladder axis ($\|b$) revealed that the as-grown $La_8Cu_7O_{19}$ crystals are semiconducting. A significant drop in the resistivity was observed upon hole doping by means of high oxygen pressure annealing, but no transition from the semiconducting behavior was observed.

ACKNOWLEDGMENTS

The authors thank Dr. Hideo Koizumi for single crystal X-ray analysis, Mr. T. Fujii for his help in resistivity measurements, and Dr. A. Maljuk for his helpful comment on the phase diagram.

REFERENCES

1. E. Dagoto and R. M. Rice, *Science* **271,** 618 (1996).
2. M. Uehara, T. Nagata, J. Akimutsu, H. Takahashi, N. Mori, and K. Kinoshita, *J. Phys. Soc. Jpn.* **65,** 2764 (1996).
3. M. Azuma, Z. Hiroi, M. Takano, K. Ishida, and Y. Kitaoka, *Phys. Rev. Lett*. **73,** 3463 (1994).
4. R. J. Cava, T. Siegrist, B. Hessen, J. J. Krajewski, W. F. Peck Jr., B. Batlogg, H. Takagi, J. V. Waszczak, L. F. Schneemeyer, and H. W. Zandbergen, *J. Solid. State Chem.* **94,** 170 (1991); *Physica C* **177,** 115 (1991).
5. B. Batlogg, R. J. Cava, L. W. Rupp Jr., J. J. Krajewski, and W. F. Peck, Jr., *Bull. Am. Phys. Soc.* **40,** 327 (1995).
6. Y. Zenitani, J. Akimutsu, H. Shibata, K. Kinoshita, and N. Mori, *in* "J. Phys. Soc. Meeting Abstracts, 1997," p. 680. [in Japanese]
7. H. Kojima and I. Tanaka, *JJAP* Series 7, 76 (1992).
8. C. Sekar, T. Watanabe, and A. Matsuda, *J. Crystal Growth* **212,** 142 (2000); Advances in Superconductivity XII: Proceedings of the 12th International Symposium on Superconductivity (ISS'99), pp. 191–193.
9. S. A. Carter, B. Batlogg, R. J. Cava, J. J. Krajewski, W. F. Peck Jr., and T. M. Rice, *Phys. Rev. Lett*. **77,** 1378 (1996).